JACS
JOURNAL OF THE AMERICAN CHEMICAL SOCIETY

ARTICLE

pubs.acs.org/JACS

Pathways for Fluorescence Quenching in 2-Aminopurine π-Stacked with Pyrimidine Nucleobases

JingXin Liang and Spiridoula Matsika*

Department of Chemistry, Temple University, Philadelphia, Pennsylvania 19122, United States

Supporting Information

ABSTRACT: Fluorescent analogues of nucleobases are very useful as probes to study DNA dynamics, because natural DNA does not fluoresce significantly. In many of these analogues, such as 2-aminopurine (2AP), the fluorescence is quenched when incorporated into DNA through processes that are not well understood. This work uses theoretical studies to examine fluorescence quenching pathways in 2AP-containing dimers. The singlet excited states of π-stacked dimer systems containing 2AP and a pyrimidine base, thymine or cytosine, have been studied using ab initio computational methods. Computed relaxation pathways along the excited-state surfaces reveal novel mechanisms that can lead to fluorescence quenching in the π-stacked dimers. The placement of 2AP on the 5′ or 3′ terminus of the dimers has different effects on the excitation energies and the relaxation pathways on the S_1 excited state. Conical intersections between the ground and first excited states exist when 2AP is placed at the 3′ side, whereas the placement of 2AP at the 5′ side leads to the switching of a bright state to a dark state. Both of these processes can lead to fluorescence quenching and may contribute to the fluorescence quenching observed in 2AP when incorporated in DNA.

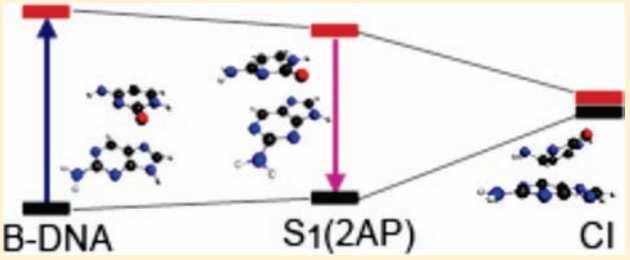

INTRODUCTION

DNA and RNA absorb UV radiation around 260 nm, but they have very low fluorescence quantum yields, because fast radiationless deactivation processes take place. These deactivation processes have been studied extensively, and they are believed to increase the photostability of DNA as it does not remain on the reactive excited state for long times.[1−3] In addition to the fact that natural DNA has a very low fluorescence quantum yield, the electronic coupling between the different bases makes the interpretation of its fluorescence very complicated.[4] The desire to use fluorescence as a sensitive spectroscopic method to monitor DNA has led to the development of fluorescent probes that can be incorporated in DNA.[5] Fluorescent base analogues are molecules that resemble the natural nucleobases, the chromophores in DNA, but small modifications in their structure render them fluorescent. Another very useful property they have is that usually they absorb and emit at wavelengths different from the natural bases, so there is no coupling with neighboring bases, and they can provide direct information about the local environment. Experimentally, fluorescent analogues of these nucleobases are used as probes to study the structure and dynamics of DNA. They are preferred over other fluorescent dyes that can be attached to DNA, because they do not disturb its structure.

2-Aminopurine (2AP) is a fluorescent analogue that is often used in the place of adenine (6-aminopurine, (A)).[6,7] Adenine and 2-aminopurine are purine derivatives and close constitutional isomers, differing only in the placement of an amino group, as shown in Figure 1. Like adenine, 2AP can form a Watson−Crick base pair with thymine and can be incorporated into nucleic acids with minimal perturbation of the overall nucleic acid structure.[8−10] For these reasons, it is a very appealing base to be used as fluorescent probe. Its spectral properties are very well characterized. It can be selectively excited at a wavelength (300−320 nm) that is red-shifted as compared to the natural DNA bases (∼260 nm). The small structural change between 2AP and A leads to distinct photophysical behavior. Experimentally, the fluorescence quantum yield of adenine is very low, 7×10^{-5},[11] and the excited-state lifetimes in aqueous environments are found to be on the order of subpicosecond.[1,2,12−14] 2AP, on the other hand, is highly emissive with a quantum yield of 0.68 in water.[6] Unlike adenine, the fluorescence of 2-aminopurine is favored by solvent polarity and has a long lifetime between 9.3 and 11.8 ns.[15,16]

The difference in photophysical behavior between isolated A and 2AP has been studied theoretically by various groups. Perun et al. used multireference methods to study both A and 2AP,[17,18] and they found that in both cases conical intersections (CIs) exist between the excited states and the ground state. CIs can facilitate radiationless decay to the ground state, which is responsible for the lack of fluorescence in adenine. Although CIs exist in 2AP also, they are inaccessible because of high barriers, and thus they cannot be efficient in quenching fluorescence. Similar conclusions were drawn by other studies.[19,20] Calculations on other fluorescent base analogues have also shown that the accessibility

Received: January 26, 2011
Published: April 12, 2011

dx.doi.org/10.1021/ja2007998 | J. Am. Chem. Soc. 2011, 133, 6799–6808

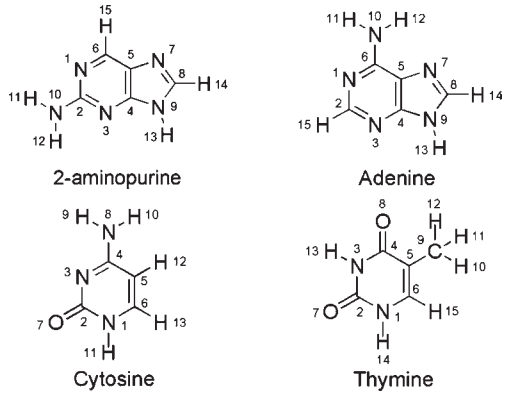

Figure 1. Structures of 2-aminopurine, adenine, cytosine, and thymine with labeling of the atoms.

of conical intersections plays the dominant role in the fluorescence versus nonradiative decay of these systems.[21,22]

While the 2AP monomer is highly fluorescent, the fluorescence of this analogue is significantly quenched when incorporated into natural DNA strands. The environmental sensitivity of 2AP makes it an excellent probe to study the effects of local conformational changes on fluorescent behavior. It has been used to study mispair recognition, base flipping, local melting, protein binding, and electron and energy transfer.[23−36] Although the fluorescence decay of 2AP in solution is single exponential, with a lifetime of ∼10 ns, dinucleotides and larger DNA fragments involving 2AP exhibit fluorescence decay that shows multiexponential decay and can be fitted to four exponential components with lifetimes of approximately <100 ps, 0.5 ns, 2 ns, and 10 ns.[23,37,38] This complex multiexponential decay seen in time-resolved fluorescence studies of 2AP-labeled DNA is attributed to the duplex existing in a multiplicity of conformational states that arise from different degrees of interbase stacking.[24,25,39−44] The shortest component is attributed to a fully stacked conformation, while the longest is due to unstacked 2AP. The fact, however, that the short components appear even in smaller oligonucleotides indicates that some quenching occurs even in cases without good interbase stacking.[37,38,45,46] Interestingly, the intensity of fluorescence of 2AP increases at 77 K,[42,47] indicating the crucial role of base motion in mediating the quenching of 2AP. The complex dynamics still exists at low temperatures, but the shortest decay component is eliminated.

The processes that contribute to the fluorescence quenching of 2AP in DNA are not well understood, although it has been shown that the quenching arises from base stacking rather than base-pairing.[23] Several mechanisms have been proposed, including photoinduced electron transfer and the presence of dark states.[32,35,46,48,49] Barton and co-workers advocate that the quenching in 2AP is caused by photoinduced electron transfer between neighboring bases, predominantly with guanine.[32,35,48,49] On the basis of the oxidation potential, guanine is the most favorable to be oxidized because it has the lowest oxidation potential of all the natural bases. Substitution of guanine by another base with unfavorable oxidation potential, inosine, slows the quenching. In contrast, other workers observe instantaneous quenching by all bases,[23,37,46] and they attribute quenching to the presence of a dark state.

Early theoretical calculations attributed the quenching to the presence of dark charge-transfer (CT) states,[50,51] where partial charge redistribution between the bases occurs. These studies, however, had used time-dependent density functional theory (TDDFT), and it is well-known now that TDDFT methods fail to compute CT states accurately,[52−54] so these results should be viewed with skepticism. Later studies using configuration interaction singles (CIS) showed that the CT states are higher energetically and are not expected to be the dominant states upon absorption.[55,56] CIS is better at predicting the relative positions between local and CT states, but it lacks electron correlation and largely overestimates excitation energies. So, the energies and importance of CT states in 2AP containing systems are still not clear.

Beyond the above limitations in previous studies of 2AP systems, the most important limitation is that static calculations using only one initial geometry at the Franck−Condon (FC) region are not sufficient to investigate fluorescence quenching mechanisms. The fate of the excited-state population after absorption is very important, and one has to consider competitive radiative and nonradiative decay mechanisms, as has been shown in the work on nucleobase monomers. Such an extensive study requires calculations of important points along the excited-state potential energy surfaces (PESs) of the systems. Extended ab initio studies of the excited states on π-stacked bases beyond the FC region are limited, mainly because of the computational cost of such calculations, and only recently have started to appear.[57−63]

In the present work, the excited-state behavior of 2AP incorporated into base stacked dimer systems is studied theoretically. We focus on two systems, 2AP with cytosine (C) and 2AP with thymine (T), where in each case 2AP is placed at the 5′ and 3′ side. We first calculate the excited states at a typical B-DNA conformation. Relaxation along the S_1 surface is then examined to study the fate of the population on this state after excitation. Two different novel mechanisms were found, and they could provide possible scenarios for fluorescence quenching.

METHODS

The initial geometries of 5′-C2AP-3′, 5′-2APC-3′, and the analogous base stacks of thymine with 2AP in B form DNA were obtained from ground-state geometries previously reported by Thompson and Hardman.[55] In that work, the geometries of the monomers had been calculated using MP2/6-31G(d,p), while the B-DNA conformations had been obtained by truncating oligomers created in Spartan.[64]

Excited-state energies and optimized structures of the monomers and dimer systems were calculated using configuration interaction singles with second order perturbation theory (CIS(2)).[65] The CIS(2) method improves upon CIS by including a Møller−Plesset second-order perturbation theory correction.[65] Others have developed similar methods,[66,67] and our version has been extended to be able to handle conical intersections between the ground and excited states. CIS(2) can be used in two forms: including the coupling with the ground state when conical intersections are sought, or omitting the coupling when better excitation energies are needed. When the coupling with the ground state is omitted, CIS(2) is similar to the quasi-degenerate CIS(D) method of Head-Gordon and co-workers,[67] the main difference being in the way one of the energy difference denominators is approximated.[65] CIS(2) without the coupling is denoted here as CIS(2X). We have shown in previous work that these methods perform well in describing conical intersections in organic molecules such as the nucleobases by comparing them to multireference methods.[65] They also describe excited states of nucleobase dimers reasonably well.[68] The CIS(2X) method was used here for single point calculations because this method is still size consistent and the coupling with the ground state is not important in that case, while the CIS(2) including the coupling was used for optimizations. Two basis sets

dx.doi.org/10.1021/ja2007998 |J. Am. Chem. Soc. 2011, 133, 6799–6808

Table 1. Vertical Excitation Energies (E in eV) and Oscillator Strengths (f) of the Monomers and Dimers Studied in This Work Calculated at the CIS(2X)/cc-pvdz+diff Level

		2AP	T	C	5′-2APT-3′	5′-T2AP-3′	5′-2APC-3′	5′-C2AP-3′
S_1	E	4.56	5.12	5.03	4.48	4.53	4.48	4.52
	f	0.1940	0.0000	0.0662	0.1610	0.1533	0.1657	0.1531
S_2	E	4.94	5.66	5.40	4.93	4.89	4.86	4.92
	f	0.0036	0.2848	0.0018	0.0039	0.0039	0.0045	0.0043
S_3	E	5.63	6.15	5.86	5.03	5.12	5.00	5.02
	f	0.0021	0.0011	0.0001	0.0001	0.0000	0.0516	0.0598
S_4	E	5.88	6.61	5.90	5.36	5.61	5.28	5.40
	f	0.1077	0.0000	0.0069	0.0064	0.0334	0.0010	0.0026
S_5	E	5.93	6.90	6.05	5.58	5.62	5.33	5.50
	f	0.0120	0.0611	0.2328	0.1590	0.1934	0.0024	0.0001
S_6	E	6.42	7.06	6.13	5.78	5.80	5.69	5.68
	f	0.0039	0.0024	0.0000	0.0188	0.0636	0.0073	0.0216
S_7	E	6.48	7.15	6.42	5.83	5.86	5.72	5.81
	f	0.0001	0.0031	0.0082	0.1018	0.0632	0.0636	0.0038

were employed, the cc-pVDZ and a modified aug-cc-pVDZ where the diffuse d functions were omitted for computational efficiency (denoted here cc-pVDZ+diff). Optimizations on the first excited-state surface (S_1) and conical intersection searches were performed at the CIS(2)/cc-pVDZ level. Natural orbitals describing the S_1 excited-state electron distribution were obtained at the CIS/cc-pVDZ level. The EOM-CCSD method with the 6-31+G* basis set was also used to calculate excited states in 2AP to compare with the CIS(2X) results.

Linearly interpolated internal coordinate (LIIC) pathways were constructed between the initial B-DNA geometries and the final optimized geometries on the S_1 surface, which provided qualitative energetic pathways between these two points. Ten geometries were created between the initial and final points. The excitation energies for each point were calculated at the CIS(2X)/cc-pVDZ+diff level. To examine the effect of stacking on the fluorescence maximum of 2AP, the S_1 excited-state minimum of 2AP was optimized at the CIS(2)/cc-pVDZ+diff level, and the optimized geometry replaced the 2AP ground-state geometry in the B-DNA dimers. These geometries are denoted S_1(2AP) in the following discussion. LIIC pathways between the S_1(2AP) $\pi\pi^*$ excited-state minimum and the final S_1 optimized geometries of the dimers were also obtained at the CIS(2X)/cc-pVDZ+diff level.

The Priroda computational packaged was used for all CIS(2) calculations.[65,69] All CIS calculations were performed using GAMESS,[70] and the EOM-CCSD calculations using the NWCHEM program.[71] Molecular orbitals were viewed using MacMolPlt.[72]

RESULTS AND DISCUSSION

2AP Monomer. Although the excited states of 2AP monomer have been studied previously, to examine how they are affected by the neighboring bases, we have recalculated their most important properties. Furthermore, comparisons with the previous theoretical and experimental results can give us a better estimate of how our methods perfom. Table 1 shows the calculated vertical excitation energies for the first seven singlet excited states of 2AP using the CIS(2X)/cc-pvdz+diff method. The two first excited states are calculated to be at 4.56 and 4.94 eV. S_1 is a $\pi\pi^*$ state with high oscillator strength $f = 0.194$, while S_2 is an $n\pi^*$ state with oscillator strength $f = 0.004$, at the CIS(2X) level. The experimental absorption maximum for 2AP in stretched films of poly(vinyl alcohol) is 4.05 eV for S_1 and 4.46 eV for S_2.[16] The EOM-CCSD/6-31+G* method predicts the first excited-state energy to be 4.39 eV, in closer agreement with experiment, and the second excited-state energy to be 4.91 eV. CIS(2X) and EOM-CCSD perform similarly, giving the absolute excitation energies to be too high by ca. 0.4 eV but the gap between S_1 and S_2 to be in close agreement with experiment. Multireference methods predict the S_1 excitation energy to be 4.18−4.19 eV and S_2 to be 4.23−4.84 eV, depending on the exact parameters for the calculation.[17,73]

We have also calculated two S_1 minima for 2AP, which had been previously predicted.[17,19,20] The adiabatic excitation energy to the $\pi\pi^*$ S_1 minimum calculated at the CIS(2X)/cc-pvdz+diff level is 4.38 eV, while the S_0-S_1 gap at that minimum corresponding roughly to a fluorescence maximum is 4.03 eV. The band origin in a resonant two-photon ionization (R2PI) spectrum of jet-cooled 2AP is 4.01 eV, again about 0.4 eV lower than our calculated number. A second $n\pi^*$ minimum also exists with adiabatic energy 4.31 eV, and S_0-S_1 gap 3.54 eV. This minimum has been restricted to planar symmetry in agreement with previous calculations.[17]

Overall, the error in our methods is comparable to the error in other high level methods that can be employed for systems of this size. As compared to experimental observables, the error is about 0.4 eV, but seems to be constant along the PES, making the method suitable for our photophysical studies where relative energies along the PES are important.

The photophysical properties of 2AP have been investigated previously.[17,19,20] It has been found that 2AP has two conical intersections between S_1 and S_0, similarly to adenine. The main difference between the two molecules that makes 2AP fluorescent while adenine is nonfluorescent is that the barriers connecting the S_1 minimum to the conical intersections are high for 2AP, almost 0.5 eV.

Absorption Spectra of B-DNA Dimers. The vertical excitation energies corresponding roughly to absorption maxima of 2AP π-stacked with the pyrimidine DNA bases cytosine and thymine have been calculated using CIS(2X)/cc-pvdz+diff. The energies are shown in Table 1. The lowest excited states of the dimers are mostly localized on each monomer, and they are somewhat perturbed as compared to the monomer excitation energies. The first excited state for all dimers is a bright state correlating to the first excited state in 2AP. This state is

dx.doi.org/10.1021/ja2007998 |J. Am. Chem. Soc. 2011, 133, 6799–6808

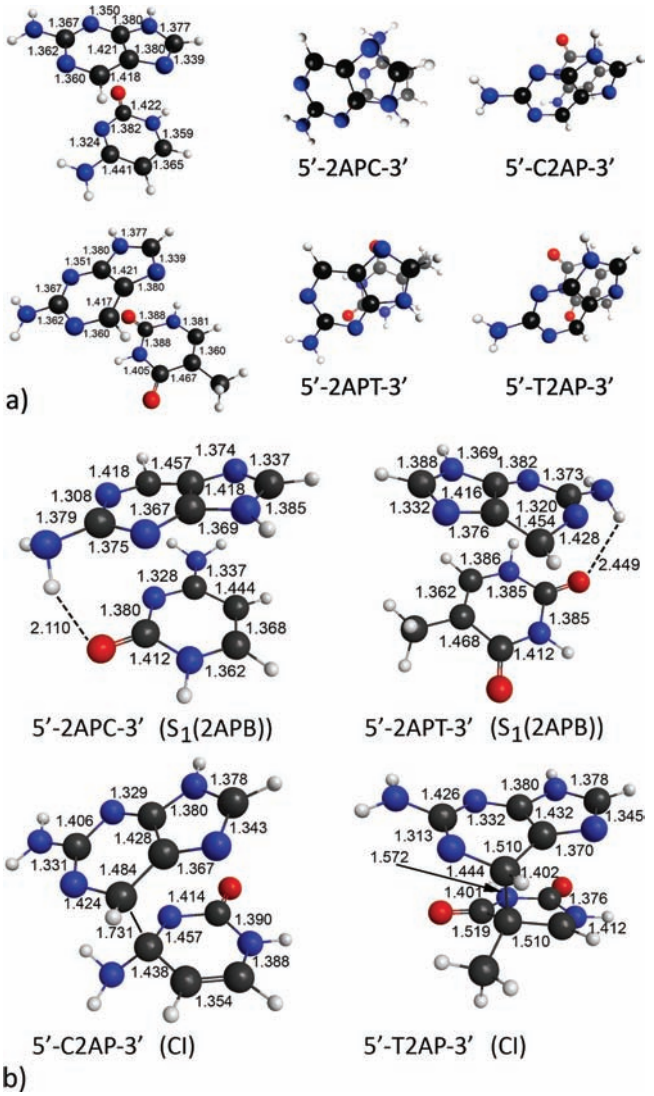

Figure 2. Geometries of the dimers at (a) the initial B-DNA structures and (b) the final points after optimization on S_1. In (a), the left side shows the bond lengths for each monomer in the dimer, while the right side shows top views. In the top view for the initial geometries, the N^1(2AP)−N^1(pyrimidine) axis is perpendicular to the plane of the paper.

red-shifted as compared to the monomer in all cases when stacked with the pyrimidine base. The red-shift is stronger when 2AP is placed at the 5′ end. For monomer 2AP, the vertical excitation energy to the first excited state is 4.56 eV. The shift is 0.08 eV for 5′-2APC-3′ and 5′-2APT-3′, while it is only 0.04 eV for 5′-C2AP-3′ and 0.03 eV for 5′-T2AP-3′. In all dimers, the oscillator strength of the bright S_1 state in the dimer is reduced as compared to the monomer, from 0.19 to 0.15−0.16. This 20% reduction in the oscillator strength indicates that the wave function/electronic distribution is affected by the interactions.

Figure 2 shows the initial structures of the dimers. The top view shows that the π-overlap and other specific interactions are different when 2AP is at the 5′ or 3′ terminus, and this could cause the different excitation energies.

The presence and importance of charge transfer excited states in DNA and in the fluorescence quenching in 2AP-containing strands has been debated extensively. Earlier theoretical work had reported the existence of CT states at low energies for stacked dimers and trimers including 2AP,[51] but later studies did not find these CT states.[55] Our results indicate that, although there is some mixing and changes in the electronic wave function of the monomer when it interacts with the other bases, pure CT states are not present within about 1 eV of the bright absorbing state, so they are not expected to play a role, at least at the initial absorption event. They could, however, become important after the initial absorption if they can be stabilized. An aspect of this will be seen later in our results.

Emission Spectra of B-DNA Dimers. The effect of π-stacking on the emission wavelengths has also been examined. The geometry of 2AP in the B-DNA conformations, which corresponds to its ground-state minimum, was replaced with the geometry of its S_1 minimum. This geometry of the dimers is denoted here S_1(2AP). For isolated 2AP, the vertical gap at this minimum, corresponding to the emission maximum, is 4.03 eV. Similarly to what was seen in absorption, π-stacking red-shifts the emission energy by a small amount. When 2AP is at the 5′ side, the red-shifts are 0.07 eV for 5′-2APT-3′ and 0.10 eV for 5′-2APC-3′. The corresponding shifts for 5′-T2AP-3′ and 5′-C2AP-3′ are 0.03 and 0.08 eV, respectively.

Yang and Stanley measured a similar effect in λ_{max} for oligonucleotides containing 2AP neighboring with different bases.[74] In an oligonucleotide containing 5′-...A-2AP-C...-3′, the fluorescence λ_{max} was 372 nm (3.33 eV), while in an oligonucleotide containing 5′-...C-2AP-A...-3′, it was 368 nm (3.37 eV). So, the difference made by the position is 0.04 eV, similar to what our calculations predict. Of course, in our calculations there is one neighbor, while in the experiments there are neighbors on both ends and there are also other bases in the sequence that will probably have some effect. Furthermore, the shifts are in general small, so general conclusions are probably inappropriate at this stage, but it is encouraging that we can predict similar trends as observed experimentally.

The position of 2AP affects not only the emission maximum but also the fluorescence quantum yield according to the same study.[74] The 5′-...A-2AP-C...-3′ probe has roughly 3 times the relative fluorescence quantum yield as compared to the 5′-...C-2AP-A...-3′ probe. As we will discuss below, our calculations show that the possible fluorescence quenching pathways depend on the position of 2AP on the 3′ or 5′ side, which could explain the observed experimental differences. The oscillator strengths at the minima for all four dimers are similar, 0.14−0.15, and they cannot explain a 3-fold difference in fluorescence quantum yield.

Sequence effects have also been reported by Rai et al.[75] when 2AP was placed in different places of DNA oligonucleotides. Among the sequences they studied, there were some where 2AP was placed either on a 5′ side of T, or on a 3′ side of T, or stacked between two thymines. The effect of the position on the emission maximum was seen to be small, on the order of 0.03 eV, as the lower values of our calculations. The important conclusion in that work was that the position of 2AP on the sequence has a great effect on energy transfer with the natural nucleobases.

Relaxing on the S_1 Potential Energy Surfaces. The mechanism for the fluorescence quenching in 2AP when incorporated into DNA continues to be an area of active debate. The involvement of dark charge transfer states has been suggested as a possible reason for the quenching, but our calculations show that at least initially these states are energetically inaccessible and the first excited state is localized on 2AP. To further investigate the quenching mechanism, we have explored the S_1 excited-state

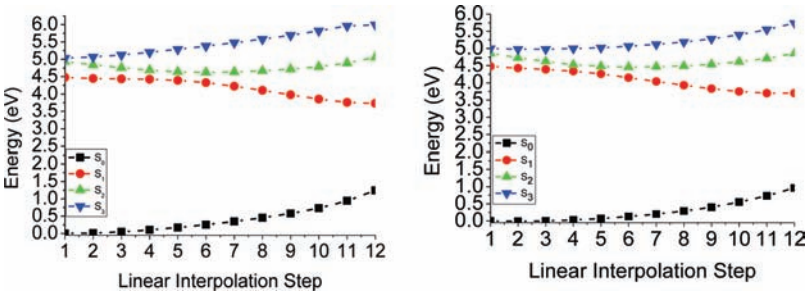

Figure 3. Energies of the S_0, S_1, S_2, S_3 excited states along the LIIC connecting the FC point to the S_1(2APB) for 5′-2APT-3′ (left panel) and 5′-2APC-3′ (right panel).

PESs, because fluorescence quenching is related to the character and dynamics of the bright excited state. The energy of the first excited bright state was minimized for the four B-DNA dimers. Interestingly, two different pathways were observed, and the outcome was quite different for the dimers with 2AP in the 5′ terminus as compared to the ones with 2AP in the 3′ terminus. Minimization of the S_1 state in 5′-2APT-3′ and 5′-2APC-3′ leads to a minimum on the S_1 surface, while minimization in 5′-T2AP-3′ and 5′-C2AP-3′ leads to a seam of conical intersections between S_0 and S_1. The details of these pathways are described below.

S_1 Dark Minimum. When the energy of the S_1 absorbing state of the dimers 5′-2APT-3′ and 5′-2APC-3′ is optimized, a minimum is reached, denoted S_1(2APB). This minimum has a small oscillator strength, so the initially bright state has been converted into a dark state. The oscillator strength is reduced from 0.16 to 0.01 in both dimers. The emission energy is considerably red-shifted as compared to absorption, 2.74 eV in 5′-2APC-3′ (2.49 eV in 5′-2APT-3′) as compared to 4.48 eV, which is the vertical excitation corresponding to the absorption maximum. The adiabatic energy is 3.70 eV in 5′-2APC-3′ and 3.73 eV in 5′-2APT-3′.

Linear interpolations between the initial FC point and S_1-(2APB) and between the monomer like fluorescent minimum S_1(2AP) and S_1(2APB) were performed to examine the accessibility of S_1(2APB). The LIIC between initial FC point and S_1(2APB) are shown in Figure 3, while the LIIC between S_1(2AP) and S_1(2APB) are given in the Supporting Information (Figure S1). In both cases, no barriers were found along the LIIC, indicating that this dark minimum is easily accessible either directly after initial excitation or after relaxation to the fluorescent minimum S_1(2AP).

The LIIC plots hint to the fact that an avoided crossing between S_1 and S_2 may exist along the paths (around point 4 of the LIICs), which could cause the switching between the bright and the dark states. To confirm this observation, we show the oscillator strengths for the first three excited states in Figure 4. This figure shows clearly that the reduction of oscillator strength is due to an avoided crossing between S_1 and S_2. Initially, S_1 is a $\pi\pi^*$ state with high oscillator strength localized on 2AP and S_2 is an $n\pi^*$ state with very small oscillator strength again localized on 2AP. While moving along the LIIC to reach the S_1(2APB), the oscillator strength for S_1 decreases steadily, while that of S_2 increases steadily. At the final point, the two states have switched character. Figure 5a,b shows the natural orbitals that describe the excitation at the first and last points of the LIIC. The natural orbitals with occupation number close to one are shown. Figure 5a shows the orbitals for 5′-2APT-3′ and 5b for 5′-2APC-3′. The left panel in each case describes the excitation for the initial FC point, while the right panel shows the orbitals involved in the excitation at S_1(2APB). It can be seen that the excitation switches from $\pi\rightarrow\pi^*$ to $n\rightarrow\pi^*$. The outcome of this avoided crossing will be fluorescence quenching because of the dark nature of the final state.

Because the excitation remains localized on 2AP at this minimum, a question that naturally arises is whether this pathway is present in 2AP monomer, and, if so, what is the reason that it does not cause fluorescence quenching in that case. If we look into the previously published studies of 2AP monomer, as was described above, we see that an $n\pi^*$ minimum exists for the monomer 2AP as well. The adiabatic energy for the monomer according to our calculations is 4.31 eV, while the emission energy is 3.54 eV. The first obvious difference between the monomer and the dimers is that the adiabatic and emission energies are much lower ($\geq$0.6 eV) for the dimers as compared to the monomer.

Figure 2b shows the geometries for S_1(2APB) for both dimers. The monomer minimum is planar, while 2AP in 5′-2APT-3′ and 5′-2APC-3′ is not planar anymore. The amino group is pyramidalized with the hydrogens pointing toward the oxygen of thymine and cytosine. Also, the $N^1C^6C^5N^7$ dihedral angle of 2AP is 15° for 5′-2APT-3′ while 8° for 5′-2APC-3′ (atom labels are shown in Figure 1). The bond lengths in the rings, however, are not very different from the monomer $n\pi^*$ minimum, because the distortions from the ground-state equilibrium structure are indicative of the lone pairs on nitrogens. Specifically, C^6N^1 on 2AP is elongated from 1.36 Å at its equilibrium structure to 1.42−1.43 Å, while C^2N^1 shortens from 1.36 to 1.31−1.32 Å. When looking at how much the overall structure has changed as compared to the initial B-DNA one, the distance between the bases is not much different from the initial, being around 3.2 Å, with the bases having approached each other somewhat. The dihedral angle H^1N^1(pyrimidine)$-N^1H^1$(2AP) defining the rotation between the bases in the double helix changes from 36° to 38° for 5′-2APT-3′, while for 5′-2APC-3′ changes from 35° to 25°, indicating that this motion has not distorted the structure expected in B-DNA significantly, especially for 5′-2APT-3′.

These comparisons indicate that the hydrogen-bonding interactions between the bases stabilize the $n\pi^*$ state as compared to the 2AP monomer. When looking at the initial geometries of the dimers in B-DNA conformation, it is clear that both 5′-2APT-3′ and 5′-2APC-3′ have the NH_2 group of 2AP in close proximity to the carbonyl group of the pyrimidine. This initiates the hydrogen-bond interaction. This hydrogen bond will be hindered in a double strand. Similar interactions between dimers of bases have

dx.doi.org/10.1021/ja2007998 |*J. Am. Chem. Soc.* 2011, 133, 6799–6808

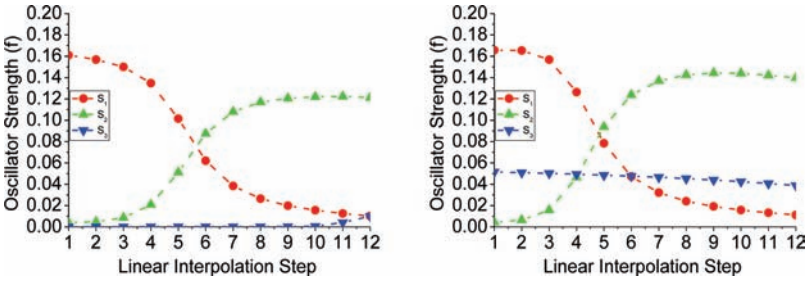

Figure 4. Oscillator strengths for S_1, S_2, S_3 along the LIIC connecting the FC point to the S_1(2APB) for 5′-2APT-3′ (left panel) and 5′-2APC-3′ (right panel).

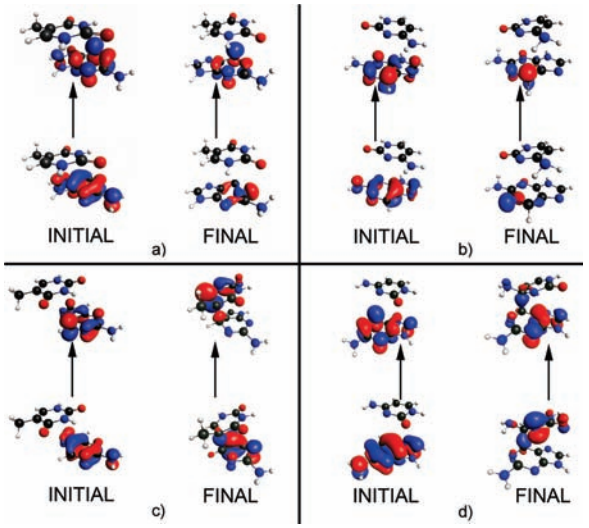

Figure 5. Natural orbitals describing the excitation of the S_1 state at the initial B-DNA geometries and at the final S_1 optimized geometries (S_1(2APB) for (a),(b) and CI for (c),(d). (a) 5′-2APT-3′, (b) 5′-2APC-3′, (c) 5′-T2AP-3′, (d) 5′-C2AP-3′. In all cases, the left side shows the orbitals initially, while the right side shows the orbitals finally.

been observed before. This intrastrand hydrogen bonding has been observed by Nachtigallova et al.[63] in a QM/MM study of a model of adenine (4-aminopyrimidine) stacked between two bases. Their conclusion is that this type of hydrogen bond may play an important role for the photodynamics within one DNA strand and that it should be of interest even in irregular segments of double-stranded nucleic acids structures.

Dual fluorescence has been observed in 2AP depending on the surrounding environment, when it is incorporated in single- and double-stranded oligonucleotides.[43,76,77] In addition to the monomer-like fluorescence at 3.35 eV, a second maximum was observed at ca. 2.75 eV. This long wavelength peak is 10 times weaker than the short wavelength. Previous work has attributed the emission to exciplex formation between 2AP and neighboring bases. Both the wavelength and the intensity of this new peak compare well with the new minimum that we have found. In the experimental work, it is proposed that the dynamical behavior of DNA can reach conformations with increased π-stacking, which will cause this long wavelength fluorescence. This argument is reinforced by the fact that the long wavelength fluorescence has also be seen in crystals, where 2AP is very efficiently π-stacked, and emits at 2.95 eV.[43] Our work shows that conformations with orientations different from regular B-DNA, but not necessarily increased π stacking, can cause a weak long wavelength fluorescence. The important point here is that weak fluorescence can occur by the local nπ^* minimum of 2AP if the interactions with neighboring bases stabilize it. There could also be other conformations besides the ones we found here that could stabilize this minimum.

Conical Intersections. Conical intersections have been previously found in all nucleobase monomers and several of their fluorescent analogues, and they are now believed to be crucial in the photophysical pathways for these systems.[78] The conical intersections can cause fluorescence quenching because of fast radiationless decay to the ground state competing with radiative decay. Could these features be responsible for the quenching in the 2AP containing dimers? Indeed, when optimizations of the S_1 PES were performed for the dimers where 2AP is at the 3′ terminus, they lead to a very small gap between S_0 and S_1. Further application of the CI search algorithm confirmed that there is a CI seam present.

LIIC plots connecting the FC point to the CI for each dimer are shown in Figure 6. LIIC plots connecting S_1(2AP) to the CI are given in the Supporting Information (Figure S2). The energy at the CI point in these plots is not exactly degenerate because the optimization was done at the CIS(2) level, while the energies shown in the figure were obtained at the CIS(2X) level. The LIIC plots indicate that there are no additional barriers to reach the CIs starting from either the FC or the fluorescent minimum S_1(2AP), and thus the CIs are easily accessible in these dimers.

The energy of the lowest energy CI on the seam in this region is about 2.8 eV above the ground-state minimum for 5′-T2AP-3′ and 3.3 eV for 5′-C2AP-3′. Because the energies of S_0 and S_1 are not degenerate at the CIS(2X) level, we report the average of their energy. In the 2AP monomer, Perun et al.[17] have shown that there are two CI seams with energies ca. 0.4 eV above the S_1 minimum, and barriers almost 0.5 eV above the S_1 minimum exist between the CIs and the S_1 minimum. These barriers and the high energy of the CIs prohibit easy accessibility of the CIs and consequent fast nonradiative decay. The CIs in the dimers, on the other hand, are energetically lower than the S_1(2AP) minima, and there are no additional barriers between the minima and the CIs, so fast nonradiative decay is expected. This is true as long as the bases are not connected by a backbone, because the backbone can add additional constraints that could make the accessibility to the CIs more difficult. The degree of flexibility of oligonucleotides will play an important role in the accessibility of these CIs.

It is again informative to compare the CIs found in the π-stacked dimers to the monomer CIs. Each monomer in the dimers has CIs between the S_1 and S_0 states, and these CIs do not

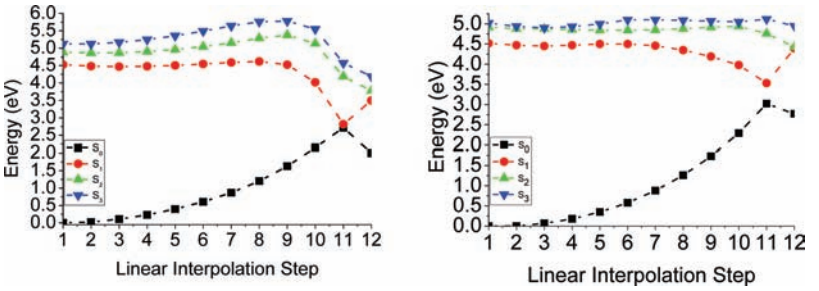

Figure 6. Energies of the S_0, S_1,S_2, S_3 excited states along the LIIC connecting the FC point to the CI for 5′-T2AP-3′ (left panel) and 5′-C2AP-3′ (right panel).

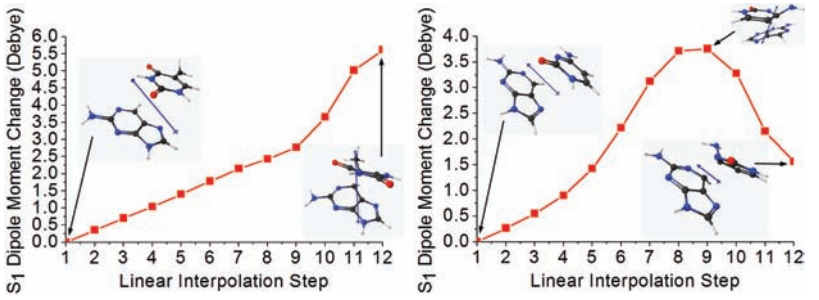

Figure 7. Magnitude of the dipole moment change for S_1 along the LIIC connecting the FC point to the CI for 5′-T2AP-3′ (left panel) and 5′-C2AP-3′ (right panel). The insets show the vector of the dipole moment at points 1 and 12 for 5′-T2AP-3′ and at points 1, 9, 12 for 5′-C2AP-3′.

disappear when the monomers are stacked. Recent dynamical studies found that the CIs are present when the bases are stacked and they still participate in the relaxation even if the steric interactions are present.[63] A closer look at the geometries and energies of the computed CIs here gives useful insight. The geometries are shown in Figure 2b. While 2AP remains relatively planar, pyramidalization of the carbon connected to the methyl group (in thymine) and to the amino group (in cytosine) occurs, resulting in extreme out-of-plane deformations of the pyrimidine bases. The two molecules approach and interact almost forming a bond between C^5 in thymine and C^6 in 2AP (1.57 Å) and between C^4 in cytosine and C^6 in 2AP (1.73 Å). The orientation of the two bases has changed as compared to the initial orientation. In 5′-C2AP-3′, the $H^1N^1(C)-N^1H^1(2AP)$ dihedral angle changes from 33° (representative of the helical twist in B-DNA) to 50°. The distance $N^9(2AP)-O^7(C)$ changes from 3.85 to 3.6 Å. Overall, the distance between the bases does not change much because part of cytosine comes closer to 2AP so that the NH_2 out-of-plane distortion is facilitated. The distortion in 5′-T2AP-3′ is larger. The $H^1N^1(T)-N^1H^1(2AP)$ dihedral angle changes from 33° to 79°. Overall, it appears that there are strong interactions between the monomers, and the CIs in the dimers are facilitated by the interaction between the monomers. There are, however, some similarities with the monomer CIs as well. The strong displacement of the amino group in cytosine and the methyl group in thymine out of the plane of the molecule is also a characteristic of the monomer CIs. The bonds in the pyrimidines are stretched very similarly to what is seen at their monomer CIs. Furthermore, the local electronic structure of the pyrimidines at these CI geometries may be the reason of the bonding interaction between the bases. Both in thymine and in cytosine monomers, the wave function has diradical character at the CI because of the twisting of the double bonds.[21,79−81] In thymine, as the C^5-C^6 double bond twists to reach the CI, the π orbital becomes more

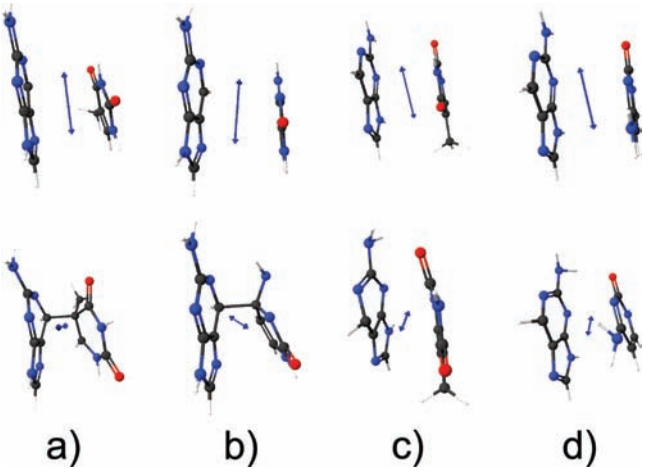

Figure 8. Transition dipole moments of the S_1 state at the initial (upper row) and final (lower row) geometries. (a) 5′-T2AP-3′, (b) 5′-C2AP-3′, (c) 5′-2APT-3′, (d) 5′-2APC-3′.

like two p-like orbitals on each carbon. Similarly, in cytosine the π orbital on N^3C^4 becomes two p-like orbitals on N^3 and C^4. This radical character on C^5 in thymine and C^4 in cytosine can facilitate the interactions with 2AP.

The character of the wave functions at the CIs is very interesting. The natural orbitals describing the excitation are shown in Figure 5c,d. The left panel in each case shows the excitation at the FC point, while the right panel shows the excitation at the CI. While initially the excitation is localized on 2AP, this is not true at the CIs for either dimer. At the CIs, the excitation involves density on both 2AP and the pyrimidine. Charge transfer character at CIs has been observed before and has been studied theoretically.[82] Strong environmental effects are

dx.doi.org/10.1021/ja2007998 |J. Am. Chem. Soc. 2011, 133, 6799–6808

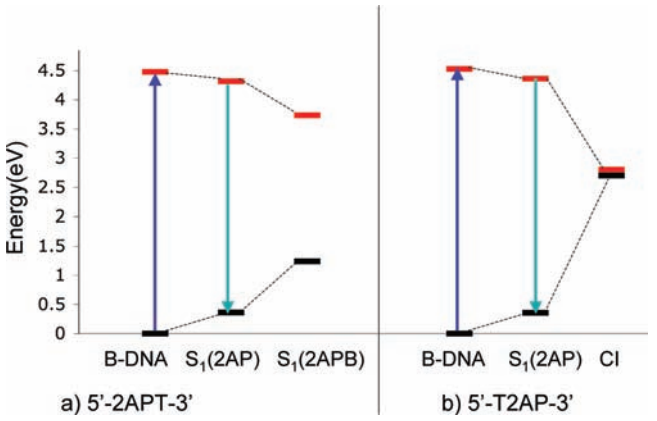

Figure 9. Energy level diagram summarizing the pathways found here that could lead to fluorescence quenching for (a) 5′-2APT-3′ and (b) 5′-T2AP-3′.

expected in these cases. Our calculations are in vacuo, but in natural systems the solvent is expected to stabilize these states and the CIs found here.

The change in the charge distribution can be clearly seen in the dipole moment change along the LIIC. Figure 7 shows the magnitude of the dipole moment change along the LIIC. This is calculated by taking the difference of the dipole moment vector at point *i*, where *i* = 1,12 in the LIIC, minus the dipole moment vector at point 1 (point 1 is always the FC point). This gives the dipole moment difference vector, and we plot the magnitude of that vector along LIIC. One sees that there is a very big difference along the path. The change in the dipole moment occurs mainly in its direction. The insets of the figure show that the direction of the dipole moment initially is along the plane of 2AP, but at the final point it is perpendicular, showing the charge transfer between the monomers. For 5′-C2AP-3′, the maximum dipole moment change occurs along the path at point 9, and then it begins declining again. One can also see that the increase in the dipole moment and charge transfer event starts immediately and increases smoothly along the path. This shows that even when absorption occurs on a locally excited state, the character of this state can change soon after absorption and delocalization and charge transfer may occur. For comparison, a similar figure of the change in the dipole moment for the 5′-2APC-3′ and 5′-2APT-3′ systems is shown in the Supporting Information (Figure S3). In that case, the dipole moment changes again because the character of the states changes, but its direction remains parallel to the plane of the molecules.

This behavior could be detected with time-resolved measurements. While stark spectroscopy can be used to detect differences in the dipole moments, such as those in Figure 7, changes in the polarization of the transition can also be important in experimental detection. Figure 8 shows the transition dipole moments for the initial and final points along the LIIC. The initial direction is always parallel to 2AP because it corresponds to a local $\pi\pi^*$ excitation on 2AP. The final direction and magnitude of the transition dipole moment vector, however, is very different. The magnitude is smaller, and the direction points between the bases, indicating the charge transfer character of the transition.

Previous experiments have proposed that population of a CT state occurs dynamically after excitation.[83] After that, the CT state is depopulated by charge recombination, which will bring the system back to its original ground state. An alternative path would lead to a pair of radical ions. Wan et al.[83] estimate the charge recombination times as the transient absorption times they measure, and they are in the range 4−85 ps depending on the bases adjacent to 2AP. In our calculations, we have examined the fate of the population after going through the CI by optimizing the ground state starting at a geometry very close to the CI. These calculations brought the bases back to their ground state, demonstrating that charge recombination occurs after passing through the CI rather than the formation of ion pairs. According to our calculations, however, there are no barriers to reach the CIs, so population of the CT state and depopulation through charge recombination should happen very fast. In fact, there is no minimum where population can be trapped leading to long lifetimes, as has been observed experimentally. One has to remember, however, that our calculations do not include the backbone or any other environmental effects, and the backbone can cause additional constrains, which could lead to barriers to reach the CI and longer time spent on a CT state.

CONCLUSIONS

We have studied four dimers, which include 2AP π-stacked with a pyrimidine base, 5′-2APT-3′, 5′-2APC-3′, 5′-T2AP-3′, and 5′-C2AP-3′, focusing on mechanisms for the observed quenching of the 2AP fluorescence. Minimizations of the S_1 state, which is initially an excitation localized on 2AP, reveal two different pathways that can lead to fluorescence quenching. Figure 9 shows a summary of the energies involved in the pathways found for the dimers of 2AP with thymine. The results are similar in cytosine as well. Initial excitation leads to the 2AP $\pi\pi^*$ bright state, which is also the fluorescent state when relaxing to its S_1(2AP) minimum. When 2AP is at the 5′ terminus, a local dark minimum is easily accessible, which reduces the radiative decay substantially. The S_1 wave function at this point is still local on 2AP, but involves different orbitals. While initially S_1 is a $\pi\pi^*$ state, it evolves into a dark minimum, which is a $n\pi^*$ state involving lone pair orbitals on 2AP. The second type of pathways is easily accessible when 2AP is at the 3′ terminus. In this case, CIs are reached, which can lead to radiationless decay. The wave function describing the S_1 state at these points involves charge transfer between the bases.

A very intriguing aspect in these findings is the large difference in the outcome when 2AP is at the 5′ versus 3′ side. Which region of the S_1 PES is stabilized depends on the interactions between the bases. The initial relaxation on the S_1 surface is governed by the forces of the 2AP localized S_1 state, because initial absorption leads to that state. There are also π interactions that move the bases with respect to each other trying to maximize the overlap. These forces are common in all dimers. As the bases approach each other, however, depending on which functional groups are closer, hydrogen-bonding interactions between the bases start to become improtant. These interactions are different depending on the position of 2AP. For 5′-2APT-3′ and 5′-2APC-3′, the carbonyls and amino group of the pyrimidines interact with hydrogen bonds with the amino group of 2AP, and these interactions stabilize the S_1 surface. For 5′-T2AP-3′ and 5′-C2AP-3′, the functional groups are further apart, and the bases rotate with respect to each other. Charge transfer is facilitated then, although it is not clear why, and the pyrimidines distort strongly reaching the points of CIs. The very different overall mechanisms highlight the importance of the interactions between the bases in determining the dominant pathways for

dx.doi.org/10.1021/ja2007998 |*J. Am. Chem. Soc.* 2011, 133, 6799–6808

excited-state dynamics. If 2AP is stacked between bases on both sides, all of the above forces will be present, and there will be competition between them. The final outcome will depend on which forces dominate.

A very important outcome of our study is that the local environment can alter the energetics of individual bases in such a way that inaccessible pathways in the monomer become accessible in the complex system. In this study, the presence of the second base, which interacted with hydrogen bonds with 2AP, altered the accessibility of the $n\pi^*$ dark state minimum. This effect, however, can happen in many other cases and could explain differences between monomers and oligomers. The outcome will depend on specific intermolecular interactions (e.g., hydrogen bonding or covalent bonding) and on the flexibility of the systems. This possibility has not been given much attention before.

On the other hand, charge transfer has been the focus in many previous studies, and it has been proposed to play an important role in 2AP quenching. The results here indicate that this can be true, however, not because a CT state is populated initially, but the locally excited state can dynamically change and acquire CT character after the initial excitation event. These results support earlier experimental discussions of CT states being populated dynamically, either in 2AP-containing oligomers or in oligomers containing only natural bases.[83,84]

In general, if we want to advance our understanding of excited states in π-stacked bases and DNA in general, we have to move beyond the initial absorption event. Exploring the PESs of the excited states beyond the FC region is essential. This has not been done extensively until now, mainly because of the computational resources that are needed for these calculations. Another approach is sampling of DNA ground-state conformations, which then is used to calculate excited states.[85] In this case, the excited-state dynamics is controlled by ground-state conformational populations. This is indeed very important because fluctuations in DNA will play a key role (shown in photochemistry as well[86]). It is not sufficient, however, to describe excited-state dynamics and reactivity in general, as the present results indicate. As discussed in the Introduction, the complex multiexponential decay in 2AP systems has been attributed to the presence of different conformational states. The various conformations may be reached because of excited-state dynamics rather than ground-state conformational sampling. This has been discussed before in the literature in dinucleotides of 2AP,[37,38] where the authors attributed some components of the multiexponential decay to excited-state dynamics rather than ground-state conformations.

Our calculations do not include the backbone connecting bases in DNA or any water molecules, so one has to be cautious about the direct applicability of the present findings in DNA. Our focus is to point out that there are different possible mechanisms that cause fluorescence quenching in stacking systems. The previous literature has focused on electron transfer or charge-transfer states. Our work shows that there exist other possibilities that have not been considered before. The accessibility of the present pathways will depend on the flexibility of the π-stacked systems containing 2AP.

■ ASSOCIATED CONTENT

Supporting Information. Figures of LIICs between S_1(2AP) and S_1(2APB) or CI. A figure of the magnitude of the dipole moment change for S_1 along the LIIC connecting the FC point to the S_1(2APB) for 5′-2APT-3′ and 5′-2APC-3′. Cartesian coordinates and energies in hartree of the geometries considered here. This material is available free of charge via the Internet at http://pubs.acs.org.

■ AUTHOR INFORMATION

Corresponding Author
smatsika@temple.edu

■ ACKNOWLEDGMENT

This work was supported by the National Science Foundation under Grant No. CHE-0911474. A portion of the research was performed using EMSL, a national scientific user facility sponsored by the Department of Energy's Office of Biological and Environmental Research and located at Pacific Northwest National Laboratory.

■ REFERENCES

(1) Cadet, J.; Vigny, P. In *Biooorganic Photochemistry*; Morrison, H., Ed.; John Wiley: New York, 1990; pp 1−272.
(2) Crespo-Hernandez, C. E.; Cohen, B.; Hare, P. M.; Kohler, B. *Chem. Rev.* **2004**, *104*, 1977.
(3) Middleton, C. T.; de La Harpe, K.; Su, C.; Law, Y. K.; Crespo-Hernandez, C. E.; Kohler, B. *Annu. Rev. Phys. Chem.* **2009**, *60*, 217–239.
(4) Markovitsi, D.; Gustavsson, T.; Vay'a, I. *J. Phys. Chem. Lett.* **2010**, *1*, 3271–3276.
(5) Wilson, J. N.; Kool, E. T. *Org. Biomol. Chem.* **2006**, *4*, 4265.
(6) Ward, D. C.; Reich, E.; Stryer, L. *J. Biol. Chem.* **1969**, *244*, 1228.
(7) Sowers, L. C.; Fazakerley, G. V.; Eritja, R.; Kaplan, B. E. *Proc. Natl. Acad. Sci U.S.A.* **1986**, *83*, 5434–5438.
(8) Evans, K.; Xu, D.; Kim, Y.; Nordlund, T. M. *J. Fluoresc.* **1992**, *2*, 209.
(9) Nordlund, T. M.; Xu, D.; Evans, K. O. *Biochemistry* **1993**, *32*, 12090.
(10) Xu, D.; Evans, K. O.; Nordlund, T. M. *Biochemistry* **1994**, *33*, 9592–9599.
(11) Onidas, D.; Markovitsi, D.; Marguet, S.; Sharonov, A.; Gustavsson, T. *J. Phys. Chem. B* **2002**, *106*, 11367.
(12) Callis, P. R. *Annu. Rev. Phys. Chem.* **1983**, *34*, 329.
(13) Daniels, M.; Hauswirth, W. *Science* **1971**, *171*, 675.
(14) Bisgaard, C. Z.; Satzger, H.; Ullrich, S.; Stolow, A. *ChemPhysChem* **2009**, *10*, 101–110.
(15) Santhosh, C.; Mishra, P. C. *Spectrochim. Acta, Part A* **1991**, *47*, 1685–1693.
(16) Holmen, A.; Norden, B.; Albinsson, B. *J. Am. Chem. Soc.* **1997**, *119*, 3114.
(17) Perun, S.; Sobolewski, A. L.; Domcke, W. *Mol. Phys.* **2006**, *104*, 1113–1121.
(18) Perun, S.; Sobolewski, A. L.; Domcke, W. *J. Am. Chem. Soc.* **2005**, *127*, 6257–6265.
(19) Seefeld, K. A.; Plützer, C.; Löwenich, D.; Häber, T.; Linder, R.; Kleinermanns, K.; Tatchen, J.; Marian, C. M. *Phys. Chem. Chem. Phys.* **2005**, *7*, 3021–3026.
(20) Serrano-Andrés, L.; Merchán, M.; Borin, A. C. *Proc. Natl. Acad. Sci. U.S.A.* **2006**, *103*, 8691–8696.
(21) Kistler, K. A.; Matsika, S. *J. Phys. Chem. A* **2007**, *111*, 2650–2661.
(22) Kistler, K. A.; Matsika, S. *Photochem. Photobiol.* **2007**, *83*, 611–624.
(23) Rachofsky, E. L.; Osman, R.; Ross, J. B. A. *Biochemistry* **2001**, *40*, 946–956.
(24) Hochstrasser, R. A.; Carver, T. E.; Sowers, L. C.; Millar, D. P. *Biochemistry* **1994**, *33*, 11971–11979.

(25) Guest, C. R.; Hochstrasser, R. A.; Sowers, L. C.; Millar, D. P. *Biochemistry* **1991**, *30*, 3271–3279.
(26) Raney, K. D.; Sowers, L. C.; Millar, D. P.; Benkovic, S. J. *Proc. Natl. Acad. Sci. U.S.A.* **1994**, *91*, 6644–6648.
(27) Su, T.-J.; Connolly, B. A.; Darlington, C.; Mallin, R.; Dryden, D. T. F. *Nucleic Acids Res.* **2004**, *32*, 2223–2230.
(28) Holz, B.; Klimasauskas, S.; Serva, S.; Weinhold, E. *Nucleic Acids Res.* **1998**, *26*, 1076–1083.
(29) Roy, S.; Lim, H. M.; Liu, M.; Sankar, A. *EMBO J.* **2004**, *23*, 869–875.
(30) Shandrick, S.; Zhao, Q.; Han, Q.; Ayida, B. K.; Takahashi, M.; Winters, G. C.; Simonsen, D. V.; Hermann, T. *Angew. Chem.* **2004**, *116*, 3239–3244.
(31) Neill, M. A. O.; Barton, J. K. *J. Am. Chem. Soc.* **2004**, *126*, 11471–11483.
(32) Kelley, S. O.; Barton, J. K. *Science* **1999**, *283*, 375.
(33) Wan, C.; Fiebig, T.; Schiemann, O.; Barton, J. K.; Zewail, A. H. *Proc. Natl. Acad. Sci. U.S.A.* **2000**, *97*, 14052–14055.
(34) Neill, M. A. O.; Becker, H.-C.; Wan, C.; Barton, J. K.; Zewail, A. H. *Angew. Chem.* **2003**, *115*, 6076–6080.
(35) Neill, M. A. O.; Becker, H.-C.; Wan, C.; Barton, J. K.; Zewail, A. H. *Angew. Chem., Int. Ed.* **2003**, *42*, 5896–5900.
(36) Nordlund, T. M. *Biochemistry* **2007**, *83*, 625–636.
(37) Somsen, O. J. G.; Keukens, L. B.; Niels de Keijzer, M.; van Hoek, A.; van Amerongen, H. *ChemPhysChem* **2005**, *6*, 1622–1627.
(38) Somsen, O. J. G.; van Hoek, A.; van Amerongen, H. *Chem. Phys. Lett.* **2005**, *402*, 61–65.
(39) Neely, R.; Daujotyte, D.; Grazulis, S.; Magennis, S.; Dryden, D.; Klimasauskas, S.; Jones, A. *Nucleic Acids Res.* **2005**, *33*, 6953–6960.
(40) Rachofsky, E. L.; Seibert, E.; Stivers, J. T.; Osman, R.; Ross, J. B. A. *Biochemistry* **2001**, *40*, 947–967.
(41) Nordlund, T.; Andersson, S.; Nilsson, L.; Rigler, R.; Graslund, A.; McLaughlin, L. *Biochemistry* **1989**, *28*, 9095–9103.
(42) Neely, R. K.; Jones, A. C. *J. Am. Chem. Soc.* **2006**, *128*, 15952–15953.
(43) Neely, R. K.; Magennis, S. W.; Parsons, S.; Jones, A. C. *ChemPhysChem* **2007**, *8*, 1095–1102.
(44) Jean, J. M.; Hall, K. B. *Biochemistry* **2004**, *43*, 10277–10284.
(45) Larsen, O. F.; van Stokkum, I. H.; Gobets, B.; van Grondelle, R.; van Amerongen, H. *Biophys. J.* **2001**, *81*, 1115–1126.
(46) Larsen, O.; van Stokkum, I.; de Weerd, F.; Vengris, M.; Aravindakumar, C.; van Grondelle, R.; Geacintov, N.; van Amerongen, H. *Phys. Chem. Chem. Phys.* **2004**, *6*, 154–160.
(47) Neill, M. A. O.; Barton, J. K. *J. Am. Chem. Soc.* **2004**, *126*, 13234–13235.
(48) Wan, C.; Fiebig, T.; Schiemann, O.; Barton, J.; Zewail, A. *Proc. Natl. Acad. Sci. U.S.A.* **2000**, *97*, 14052–14055.
(49) Fiebig, T.; Wan, C.; Zewail, A. *ChemPhysChem* **2002**, *3*, 781–788.
(50) Jean, J. M.; Hall, K. B. *Biochemistry* **2002**, *41*, 13152–13161.
(51) Jean, J. M.; Hall, K. B. *Proc. Natl. Acad. Sci. U.S.A.* **2001**, *98*, 37–41.
(52) Dreuw, A.; Head-Gordon, M. *Chem. Rev.* **2005**, *105*, 4009–4037.
(53) Dreuw, A.; Weisman, J. L.; Head-Gordon, M. *J. Chem. Phys.* **2003**, *119*, 2943.
(54) Lange, A.; Rohrdanz, M.; Herbert, J. M. *J. Phys. Chem. B* **2008**, *112*, 6304.
(55) Hardman, S. J. O.; Thompson, K. C. *Biochemistry* **2006**, *45*, 9145–9155.
(56) Hardman, S. J. O.; Thompson, K. C. *Int. J. Quantum Chem.* **2007**, *107*, 2092–2099.
(57) Boggio-Pasqua, M.; Groenhof, G.; Schäfer, L. V.; Brubmüller, H.; Robb, M. A. *J. Am. Chem. Soc.* **2007**, *129*, 10996–10997.
(58) Blancafort, L.; Migani, A. *J. Am. Chem. Soc.* **2007**, *129*, 14540–14541.
(59) Roca-Sanjuán, D.; Olaso-González, G.; González-Ramírez, I.; Serrano-Andrés, L.; Merchán, M. *J. Am. Chem. Soc.* **2008**, *130*, 10768.
(60) Serrano-Pérez, J. J.; González-Ramírez, I.; Coto, P. B.; Merchán, M.; Serrano-Andrés, L. *J. Phys. Chem. B* **2008**, *112*, 14096–14098.
(61) Olaso-González, G.; Merchán, M.; Serrano-Andrés, L. *J. Am. Chem. Soc.* **2009**, *131*, 4368–4377.
(62) Santoro, F.; Barone, V.; Improta, R. *J. Am. Chem. Soc.* **2009**, *131*, 15232–15245.
(63) Nachtigallova, D.; Zeleny, T.; Ruckenbauer, M.; Mueller, T.; Barbatti, M.; Hobza, P.; Lischka, H. *J. Am. Chem. Soc.* **2010**, *132*, 8261.
(64) *Wavefunction. Spartan 02*; Wavefunction, Inc.: California, USA, 2002.
(65) Laikov, D.; Matsika, S. *Chem. Phys. Lett.* **2007**, *448*, 132–137.
(66) Head-Gordon, M.; Rico, R. J.; Oumi, M.; Lee, T. J. *Chem. Phys. Lett.* **1994**, *219*, 21–29.
(67) Head-Gordon, M.; Oumi, M.; Maurice, D. *Mol. Phys.* **1999**, *96*, 593.
(68) Kozak, C.; Lu, K. A. K. Z.; Matsika, S. *J. Phys. Chem. B* **2010**, *114*, 1674.
(69) Laikov, D. *Priroda: An Electronic Structure Code*, Version 7; 2007.
(70) Schmidt, M. W.; Baldridge, K. K.; Boatz, J. A.; Elbert, S. T.; Gordon, M. S.; Jensen, J. H.; Koseki, S.; Matsunaga, N.; Nguyen, K. A.; Su, S.; Windus, T. L.; Dupuis, M.; Montgomery, J. A. *J. Comput. Chem.* **1993**, *14*, 1347.
(71) *High Performance Computational Chemistry Group, NWChem, a Computational Chemistry Package for Parallel Computers, Version 4.5*; Pacific Northwest National Laboratory: Richland, WA, 2003.
(72) Bode, B. M.; Gordon, M. S. *J. Mol. Graphics Modell.* **1999**, *16*, 133–138.
(73) Mburu, E.; Matsika, S. *J. Phys. Chem. A* **2008**, *112*, 12485–12491.
(74) Yang, K. S.; Stanley, R. J. *Biochemistry* **2006**, *45*, 11239–11245.
(75) Rai, P.; Cole, T. D.; Thompson, E.; Millar, D. P.; Linn, S. *Nucleic Acids Res.* **2003**, *31*, 2323–2332.
(76) Rist, M.; Wagenknecht, H.-A.; Fiebig, T. *ChemPhysChem* **2002**, *3*, 704.
(77) Bonnist, E. Y. M.; Jones, A. C. *ChemPhysChem* **2008**, *9*, 1121–1129.
(78) Kistler, K. A.; Matsika, S. In *Challenges and Advances in Computational Chemistry and Physics: Multi-scale Quantum Models for Biocatalysis: Modern Techniques and Applications*; Lee, T.-S., York, D. M., Eds.; Springer Verlag: Netherlands, 2009; Vol. 7, pp 285−339.
(79) Perun, S.; Sobolewski, A. L.; Domcke, W. *J. Phys. Chem. A* **2006**, *110*, 13238.
(80) Merchán, M.; Gonzalez-Luque, R.; Climent, T.; Serrano-Andrés, L.; Rodriuguez, E.; Reguero, M.; Pelaez, D. *J. Phys. Chem. B* **2006**, *110*, 26471–26476.
(81) Zgierski, M. Z.; Patchkovskii, S.; Fujiwara, T.; Lim, E. C. *J. Phys. Chem. A* **2005**, *109*, 9384–9387.
(82) Burghardt, I.; Hynes, J. T. *Mol. Phys.* **2006**, *104*, 903–914.
(83) Wan, C.; Xia, T.; Becker, H.-C.; Zewail, A. *Chem. Phys. Lett.* **2005**, *412*, 158–163.
(84) Takaya, T.; Su, C.; de La Harpe, K.; Crespo-Hernandez, C. E.; Kohler, B. *Proc. Natl. Acad. Sci. U.S.A.* **2008**, *105*, 10285–10290.
(85) McCullagh, M.; Hariharan, M.; Lewis, F. D.; Markovitsi, D.; Douki, T.; Schatz, G. C. *J. Phys. Chem. B* **2010**, *114*, 5215–5221.
(86) Schreier, W. J.; Schrader, T. E.; Koller, F. O.; Gilch, P.; Crespo-Hernandez, C. E.; Swaminathan, V. N.; Carell, T.; Zinth, W.; Kohler, B. *Science* **2007**, *315*, 625–629.